Acta Crystallographica Section A
Foundations of Crystallography
ISSN 0108-7673

Received 14 December 2000
Accepted 22 March 2001

Analysis of chord-length distributions

C. Burger[a]*† and W. Ruland[b]

[a]Max-Planck-Institut für Kolloid- und Grenzflächenforschung, D-14424 Potsdam, Germany, and [b]Philipps-Universität Marburg, Fachbereich Chemie, D-35032 Marburg, Germany. Correspondence e-mail: cburger@sunysb.edu

© 2001 International Union of Crystallography
Printed in Great Britain – all rights reserved

A closed-form analytical solution for the inversion of the integral equation relating small-angle scattering intensity distributions of two-phase systems to chord-length distributions is presented. The result is generalized to arbitrary derivatives of higher order of the autocorrelation function and to arbitrary projections of the scattering intensity (including slit collimation). This inverse transformation offers an elegant way to investigate the impact of certain features, *e.g.* singularities, in the chord-length distribution or its higher-order derivatives on the scattering curve, *e.g.* oscillatory components in the asymptotic behavior at a large scattering vector. Several examples are discussed.

1. Introduction

Chord-length distributions (CLD) play an important role in the qualitative and quantitative evaluation of the small-angle scattering (SAS) of two-phase systems, in both the dilute and the dense case (Méring & Tchoubar-Vallat, 1965, 1966; Porod, 1967; Méring & Tchoubar, 1968; Wu & Schmidt, 1971). The relationship between the CLD $g(r)$ and the autocorrelation function (CF) $\gamma(r)$ is given by

$$g(r) = l_p \gamma''(r > 0), \qquad (1)$$

where l_p is the average chord length (Porod length). The CLD contains the complete structural information obtainable from non-normalized SAS intensities of statistically isotropic two-phase systems.

The behavior of $g(r)$ in the vicinity of small r is defined by the general structure of the interface (edges, vertices, curvature; Ciccariello *et al.*, 1981; Ciccariello & Benedetti, 1982; Ciccariello, 1993; Sobry *et al.*, 1994; Ciccariello & Sobry, 1995). Singularities in g and g' at finite values of r are related to particularities of the surface in the vicinity of minimal or maximal diameter of monodisperse particles in dilute solution (Wu & Schmidt, 1974) or of the structural unit in periodic dense two-phase systems, respectively.

In the case of lamellar two-phase systems, the appropriate one-dimensional equivalent of the CLD to be used for the evaluation of structural parameters is the interface distribution function (Ruland, 1977, 1978).

The CLD is determined by the integral transform (Méring & Tchoubar-Vallat, 1965, 1966)

$$g(r) = -8 \int\limits_0^\infty [1 - 2\pi^3 s^4 l_p k^{-1} I(s)] \left(\frac{\sin(z)}{z}\right)'' \mathrm{d}s, \qquad (2)$$

where I is the SAS intensity (in unsmeared pin-hole collimation), $s = 2\lambda^{-1}\sin\theta$ is the absolute value of the scattering vector, 2θ the scattering angle, λ the wavelength, k is a normalization factor (Porod invariant), $z = 2\pi rs$ and the derivatives of $\sin(z)/z$ are with respect to z.

The possibility of an inversion of (2), *i.e.* the integral transform to be used to obtain $I(s)$ from $g(r)$, has been discussed by Méring & Tchoubar (1968), but an explicit expression for this transform was not found by those authors.

In this study, we present a closed-form solution to a generalization of this problem, namely the transformation of $\gamma^{(n)}(r)$ for arbitrary n (which can be specialized to $n = 2$, but is also valid for $n = 0$) to an arbitrary projection of the corresponding scattering curve (so that slit-smeared scattering curves in the infinite-slit-length approximation are also included in the approach). Examples of its application are given that demonstrate the usefulness of this transformation for the solution of various problems.

The paper closes with a short review of the requirements for an accurate determination of $g(r)$ from experimental data.

2. Basic relationships

For the purpose of the mathematical treatment developed in this paper, we consider the function $\gamma(r)$ to be defined for positive values of r only, and continuously differentiable at $r = 0$. It is shown in Appendix *A* that this definition of $\gamma(r)$ does not restrict the information contained in $\gamma(r)$ if the appropriate transforms are used.

We start with the relationship

$$I(s) = k \int\limits_0^\infty \gamma(r) \frac{\sin(z)}{z} 4\pi r^2 \,\mathrm{d}r, \qquad (3)$$

where $k = V\phi(1-\phi)(\rho_1 - \rho_2)^2$ (Porod, 1951, 1952*a*,*b*) and V is the irradiated volume of the sample, ρ_j is the (constant)

† Present address: Department of Chemistry, State University of New York at Stony Brook, Stony Brook, NY 11794, USA.

Table 1
The kernels $K_{1,n}^{-1}$ and $K_{3,n}^{-1}$ for n up to 4.

n	$K_{1,n}^{-1}$	$K_{3,n}^{-1}$
0	$\cos z$	$z^{-1}\sin z$
1	$-\sin z$	$z^{-2}(z\cos z - \sin z)$
2	$1-\cos z$	$z^{-2}(2-2\cos z - z\sin z)$
3	$-z+\sin z$	$z^{-2}(-2z+3\sin z - z\cos z)$
4	$-1+z^2/2+\cos z$	$z^{-2}(-4+z^2+4\cos z + z\sin z)$

Table 2
The kernel $K_{2,n}^{-1}$ for n up to 4.

n	$K_{2,n}^{-1}$
0	$J_0(z)$
1	$-J_1(z)$
2	$(\pi/2)[J_1(z)\mathbf{H}_0(z) - J_0(z)\mathbf{H}_1(z)]$
3	$-zJ_0(z)+2J_1(z)-(\pi z/2)[J_1(z)\mathbf{H}_0(z)-J_0(z)\mathbf{H}_1(z)]$
4	$(z^2/2)J_0(z)-(z/2)J_1(z)-(\pi/4)(3-z^2)[J_1(z)\mathbf{H}_0(z)$ $-J_0(z)\mathbf{H}_1(z)]$

electron density (small-angle X-ray scattering, SAXS) or scattering-length density (small-angle neutron scattering, SANS) within phase j and ϕ is the volume fraction of one phase. This definition of k implies that the interfacial boundaries of the phases are infinitely sharp.

If we designate a d-dimensional projection by $\{\ \}_d$, we obtain

$$\{I\}_2(s) = 2\int_0^\infty I(s^2+y^2)^{1/2}\,\mathrm{d}y = 2\pi k\int_0^\infty r\gamma(r)J_0(z)\,\mathrm{d}r \tag{4}$$

and

$$\{I\}_1(s) = 2\pi\int_0^\infty yI(s^2+y^2)^{1/2}\,\mathrm{d}y = 2k\int_0^\infty \gamma(r)\cos(z)\,\mathrm{d}r, \tag{5}$$

where J_0 is the Bessel function of the first kind of zero order. $\{I\}_2$ is equivalent to the SAS intensity measured with a slit system of 'infinite' length. $\{I\}_1$ is related to the lattice size component of a Debye–Scherrer line profile.

If we simplify the notation by putting $k=1$, $I_3 = I$, $I_2 = \{I\}_2$ and $I_1 = \{I\}_1$, we find the general expression

$$I_d(s) = \int_v \gamma(r)K_d(z)\,\mathrm{d}v_{d,r}, \tag{6}$$

where K_d is the general transformation kernel

$$K_d(z) = \Gamma(d/2)(z/2)^{1-d/2}J_{d/2-1}(z) \tag{7}$$

and the volume element in d-dimensional space is given by

$$\mathrm{d}v_{d,r} = \frac{2\pi^{d/2}}{\Gamma(d/2)}r^{d-1}\,\mathrm{d}r. \tag{8}$$

The inversion of (6) is

$$\gamma(r) = \int_v I_d(s)K_d(z)\,\mathrm{d}v_{d,s}, \tag{9}$$

where $\mathrm{d}v_{d,s}$ is the reciprocal-space analog to $\mathrm{d}v_{d,r}$.

3. Relationship between I_d and the derivatives of γ

From (9), we obtain

$$\gamma^{(n)}(r) = \int_v (2\pi s)^n I_d(s)K_d^{(n)}(z)\,\mathrm{d}v_{d,s}, \tag{10}$$

where the superscript (n) represents the nth derivative with respect to r or z, respectively.

For the inversion of the integral transform (10), we expect a relationship of the type

$$(2\pi s)^n I_d(s) = \int_v \gamma^{(n)}(r)K_{d,n}^{-1}(z)\,\mathrm{d}v_{d,r}, \tag{11}$$

where $K_{d,n}^{-1}$ is the inverse kernel to $K_d^{(n)}$. It is shown in Appendix *A* that a general expression for the inverse kernel can be found:

$$K_{d,n}^{-1}(z) = \frac{(-z)^n}{(d)_n}\,{}_1F_2\left(\left.\begin{matrix}(1+d)/2\\(d+n)/2,\,(1+d+n)/2\end{matrix}\right| -\frac{z^2}{4}\right), \tag{12}$$

where $(d)_n = \Gamma(d+n)/\Gamma(d)$ is the Pochhammer symbol and ${}_1F_2$ is a hypergeometric function. Tables 1 and 2 show explicit expressions for $d = 1, 2, 3$, and values of n up to 4.

For odd values of d, the inverse kernel is composed of trigonometric functions. Even values of d result in combinations of Bessel functions J_ν and Struve functions $\mathbf{H}_\nu$, both of the first kind.

It is readily verified that the inverse kernels $K_{d,n}^{-1}$ follow a three-termed recurrence relation

$$K_{d,n}^{-1}(z) = -(n-2)^{-1}[zK_{d,n-1}^{-1}(z) + (d+n-3)K_{d,n-2}^{-1}(z) + zK_{d,n-3}^{-1}(z)], \tag{13}$$

which can be used for $n > 2$ to extend these tables. It should also be noted that symbolic software packages such as *Mathematica* or *Maple* have no problems finding explicit expressions for specified d and n.

However, especially for the case where $n = 2$, the practical use of these explicit expressions is limited since the computational effort of calculating a single Struve $\mathbf{H}_\nu$ function, being itself a hypergeometric function of the ${}_1F_2$ type, is comparable to calculating the complete $K_{2,n}^{-1}$ kernel using the generic expression (12), and analytical properties such as asymptotic expansions are also better investigated with the generic kernel.

The equivalent of the integral transform (10) has been discussed by Méring & Tchoubar (1968) and the problem of its inversion has been mentioned, but a solution was not found. A similar problem has been considered by Ciccariello (1995) for the case $d = 3$ and odd n which can be reformulated in the form (11). A solution has been given, but it is complicated and lengthy. The general kernel of the inverse transformation (11), especially presented in its concise form (12), has been unknown until now.

4. Relationship between I_d and the chord-length distribution

The relationship between γ and the chord-length distribution g (Méring & Tchoubar-Vallat, 1965, 1966, Méring & Tchoubar, 1968) is given by (1). The Porod length l_p is the average chord length of the two-phase system defined by

$$l_p = \int_0^\infty l\, g(l)\,\mathrm{d}l = (\langle l_1\rangle^{-1} + \langle l_2\rangle^{-1})^{-1}, \tag{14}$$

where $\langle l_j\rangle$ is the number average of the chord length within phase j.

The non-oscillatory component in $K_{d,2}^{-1}$ is related to the Porod asymptote. We consider the relationship

$$\begin{aligned}(2\pi s)^2 I_3(s) &= \int_v \gamma''(r) K_{3,2}^{-1}(z)\,\mathrm{d}v_{d,r} \\ &= \int_v \gamma''(r)\frac{2}{z^2}\,\mathrm{d}v_{d,r} \\ &\quad - \int_v \gamma''(r)\frac{1}{z^2}(2\cos z + z\sin z)\,\mathrm{d}v_{d,r} \\ &= \frac{2}{\pi s^2 l_p}\left[\int_0^\infty g(r)\,\mathrm{d}r - \int_0^\infty g(r)\left(\cos z + \frac{z}{2}\sin z\right)\mathrm{d}r\right].\end{aligned} \tag{15}$$

Since, by definition,

$$\int_0^\infty g(r)\,\mathrm{d}r = 1, \tag{16}$$

we obtain

$$2\pi^3 s^4 I_3(s) = l_p^{-1}[1 - G_3(s)]. \tag{17}$$

From (17) and (15), we find Porod's law (Porod, 1952*a*,*b*) for I_3:

$$\lim_{s\to\infty} 2\pi^3 s^4 I_3(s) = 1/l_p \tag{18}$$

and the relationship

$$\begin{aligned}G_3(s) &= 1 - 2\pi^3 s^4 l_p I_3(s) \\ &= \int_0^\infty g(r)[1 - (z^2/2)K_{3,2}^{-1}(z)]\,\mathrm{d}r,\end{aligned} \tag{19}$$

which is the inversion of the relationship

$$g(r) = -8\int_0^\infty G_3(s) K_3''(z)\,\mathrm{d}s. \tag{20}$$

For arbitrary values of d, the non-oscillatory component of $K_{d,2}^{-1}(z)$ is $\Gamma(d)z^{1-d}$. This leads to

$$\begin{aligned}G_d(s) &= 1 - \frac{2\pi^{(3+d)/2}s^{1+d}}{\Gamma[(1+d)/2]} l_p I_d(s) \\ &= \int_0^\infty g(r)\left[1 - \frac{z^{d-1}}{\Gamma(d)}K_{d,2}^{-1}(z)\right]\mathrm{d}r,\end{aligned} \tag{21}$$

which is the inversion of the integral transform

$$g(r) = -\frac{4\pi^{1/2}\Gamma[(1+d)/2]}{\Gamma(d/2)}\int_0^\infty G_d(s) K_d''(z)\,\mathrm{d}s. \tag{22}$$

For arbitrary values of d, Porod's law is given by

$$\lim_{s\to\infty}\frac{2\pi^{(3+d)/2}s^{1+d}}{\Gamma[(1+d)/2]} I_d(s) = \frac{1}{l_p}. \tag{23}$$

The equivalent of the integral transform (22) for $d = 1, 2, 3$ has already been given by Méring & Tchoubar (1968), whereas the inverse transform (21) has been unknown until now.

5. Applications

5.1. Spheres

We consider the CF of a sphere of diameter D and its higher-order derivatives with respect to $x = r/D$:

$$\gamma_s = \left(1 - \frac{3x}{2} + \frac{x^3}{2}\right)\theta(1-x) \tag{24}$$

$$\gamma_s'' = 3x\theta(1-x) \tag{25}$$

$$\gamma_s^{(3)} = 3[\theta(1-x) - \delta(1-x)] \tag{26}$$

$$\gamma_s^{(4)} = -3[\delta(1-x) + \delta'(1-x)]. \tag{27}$$

θ is the Heaviside unit-step function [$\theta'(x) = \delta(x)$] and δ the Dirac δ function. Equations (24)–(27) provide an instructive example how to apply the inverse transformation if singularities are present which can be reduced to δ functions upon multiple differentiation. As our inverse transformation (11) holds for arbitrary differentiation order n, we are at liberty to differentiate our CF or CLD as often as we wish until the resulting $\gamma^{(n)}$ is in a form suitable to perform the integration. Since an integration over a δ function trivially reduces to the kernel, $\int\delta(x-t)K(t)\,\mathrm{d}t = K(x)$, δ functions are preferred targets for this multiple differentiation process. If we encounter a situation where $\gamma^{(n)}$ consists of a linear combination of terms where their δ functions appear at different n, like it is in (26) and (27), we may even split this linear combination into single terms and *treat each term separately with a different n*, this technique being justified by the fact that both the differentiation as well as our inverse integral transform are linear operations. While we believe this intuitive argument is rigorous and, thus, sufficient, the same result can also be shown in a more formal way involving integration by parts. Hence, applying (11) to the δ terms ('δ shells') in $\gamma_s^{(3)}$ and $\gamma_s^{(4)}$, we obtain

$$I_{s,d} = -\frac{6\pi^{d/2}D^d}{\Gamma(d/2)}[z^{-3}K_{d,3}^{-1}(z) + z^{-4}K_{d,4}^{-1}(z)], \tag{28}$$

where $z = 2\pi Ds$. For $d = 3$, this reduces to the well known Rayleigh expression for the scattering of a sphere. For $d = 2$, we obtain an analytical expression for the scattering of a sphere using infinite slit collimation.

Clearly, the sphere represents a special case, since its CLD can be completely reduced to δ functions so that the exact solution for the scattering curve can be expressed in terms of inverse kernels. In the general case, there will be additional terms which cannot be reduced to δ functions. In this case, δ functions can only be produced at the singularites of the CLD and the application of the described technique to only these δ terms leads to the asymptotic behavior of the scattering curve.

5.2. Ellipsoids of revolution

The first oscillatory components of the SAS of an ellipsoid of revolution have been derived by Wu & Schmidt (1973*a*). In this section, we show a way to determine all components of the asymptotic behavior of the SAS.

The direction-dependent CF of an ellipsoid of revolution $\gamma_e(\mathbf{x})$ is obtained from the CF of a sphere by an affine deformation

$$\gamma_e(\mathbf{x}) = \gamma_s(\mathbf{Tx}) \tag{29}$$

using the tensor

$$\mathbf{T} = \begin{pmatrix} \lambda^{1/2} & & \\ & \lambda^{1/2} & \\ & & 1/\lambda \end{pmatrix}. \tag{30}$$

Since $x = r/D$ and $\det \mathbf{T} = 1$, the volume of the ellipsoid is equal to that of the corresponding sphere ($V = \pi D^3/6$) independent of the deformation parameter λ. The semiaxes of the ellipsoid are $a = b = D/(2\lambda^{1/2})$ and $c = \lambda D/2$; $\lambda < 1$ defines a prolate, $\lambda > 1$ an oblate ellipsoid, respectively.

Using polar coordinates (polar angle ϕ, $\zeta = \cos\phi$), we find

$$\gamma_e(\mathbf{x}) = \gamma_s[xf(\zeta)], \tag{31}$$

where

$$f(\zeta) = [\lambda - \zeta^2(\lambda - \lambda^{-2})]^{1/2}. \tag{32}$$

The third and fourth derivatives of γ_e with respect to x are

$$\gamma_e^{(3)}(x,\zeta) = -3[f(\zeta)]^3\{\delta[1 - xf(\zeta)] - x\theta[1 - xf(\zeta)]\} \tag{33}$$

$$\gamma_e^{(4)}(x,\zeta) = -3[f(\zeta)]^3\{\delta'[1 - xf(\zeta)] + f(\zeta)\delta[1 - xf(\zeta)]\}. \tag{34}$$

The δ terms ('δ shells') in (33) and (34) are

$$[\gamma_e^{(3)}(x,\zeta)]_\delta = -3[f(\zeta)]^3\delta[1 - xf(\zeta)] \tag{35}$$

$$[\gamma_e^{(4)}(x,\zeta)]_\delta = -3[f(\zeta)]^4\delta[1 - xf(\zeta)]. \tag{36}$$

The spherical average is obtained by (note that $d\zeta = -\sin\phi\, d\phi$)

$$\langle\gamma_e^{(n)}(x,\zeta)\rangle_\omega \equiv \gamma_e^{(n)}(x) = \tfrac{1}{2}\int_{-1}^{1} \gamma_e^{(n)}(x,\zeta)\, d\zeta. \tag{37}$$

For the spherical average of the δ shell in $\gamma_s^{(3)}$, we find the expressions

$$\begin{aligned}[\gamma_e^{(3)}(x)]_\delta &= -\frac{3\lambda}{x^4[(\lambda^3-1)(\lambda x^2-1)]^{1/2}} \\ &\quad\times \theta[(x-\lambda^{-1/2})(\lambda - x)] \\ &= -\frac{3\lambda^{1/2}\exp\{\pi i(\operatorname{sgn}[\lambda-1]-1)/4\}}{x^4|\lambda^3-1|^{1/2}[(x+\lambda^{-1/2})(x-\lambda^{-1/2})]^{1/2}} \\ &\quad\times \theta[(x-\lambda^{-1/2})(\lambda - x)].\end{aligned} \tag{38}$$

The spherical average of the δ shell in $\gamma_e^{(4)}$ is given by

$$[\gamma_e^{(4)}(x)]_\delta = \frac{1}{x}[\gamma_e^{(3)}(x)]_\delta. \tag{39}$$

Applying (11) to the δ shells in $\gamma_e^{(3)}$ and $\gamma_e^{(4)}$ and introducing the parameter $y = Ds$, we obtain

$$\begin{aligned}I_{e,3}(y) &= \frac{4\pi}{(2\pi y)^4}\int_{\lambda^{-1/2}}^{\lambda} x^2[\gamma_e^{(3)}(x)]_\delta \\ &\quad\times\left[2\pi y K_{33}^{-1}(2\pi xy) + \frac{1}{x}K_{34}^{-1}(2\pi xy)\right] dx \\ &= \frac{1}{(2\pi y)^4}\int_{\lambda^{-1/2}}^{\lambda}[\gamma_e^{(3)}(x)]_\delta F(x,y)\, dx,\end{aligned} \tag{40}$$

where

$$\begin{aligned}F(x,y) &= 4\pi x^2\left[2\pi y K_{33}^{-1}(2\pi xy) + \frac{1}{x}K_{34}^{-1}(2\pi xy)\right] \\ &= -4\pi x - \frac{4}{\pi x y^2} - 4\pi x\cos(2\pi xy) \\ &\quad + \frac{4\cos(2\pi xy)}{\pi x y^2} + \frac{8\sin(2\pi xy)}{y}.\end{aligned} \tag{41}$$

From the first non-oscillatory term of $F(x, y)$, we obtain the Porod term $I_{e,3,P}$:

$$\begin{aligned}I_{e,3,P}(y) &= \frac{1}{(2\pi y)^4}\left(-4\pi\int_{\lambda^{-1/2}}^{\lambda} x[\gamma_e^{(3)}(x)]_\delta\, dx\right) \\ &= \frac{3}{8\pi^3 y^4}\left[\frac{1}{\lambda} + \frac{\lambda^2}{(\lambda^3-1)^{1/2}}\arccos(\lambda^{-3/2})\right].\end{aligned} \tag{42}$$

Accordingly, the average chord length is

$$l_p = \frac{4D}{3}\left[\frac{1}{\lambda} + \frac{\lambda^2}{(\lambda^3-1)^{1/2}}\arccos(\lambda^{-3/2})\right]^{-1}. \tag{43}$$

From the second non-oscillatory term of $F(x, y)$, we obtain the Kirste & Porod (1962) term $I_{e,3,\mathrm{KP}}$:

$$\begin{aligned}I_{e,3,\mathrm{KP}}(y) &= \frac{1}{(2\pi y)^4}\left(-\frac{4}{\pi y^2}\int_{\lambda^{-1/2}}^{\lambda}[\gamma_e^{(3)}(x)]_\delta\,\frac{dx}{x}\right) \\ &= \frac{3}{32\pi^5 y^6}\left[3 + \frac{2}{\lambda^3} + \frac{3\lambda^3}{(\lambda^3-1)^{1/2}}\arccos(\lambda^{-3/2})\right].\end{aligned} \tag{44}$$

The oscillatory terms $I_{e,3,\mathrm{osc}}$ are given by the integral transform

$$\begin{aligned}I_{e,3,\mathrm{osc}}(y) &= \frac{1}{(2\pi y)^4}\int_{\lambda^{-1/2}}^{\lambda}[\gamma_e^{(3)}(x)]_\delta \\ &\quad\times\left[-4\pi x\cos(2\pi xy) + \frac{4\cos(2\pi xy)}{\pi x y^2} \right.\\ &\quad\left. + \frac{8\sin(2\pi xy)}{y}\right] dx,\end{aligned} \tag{45}$$

which results in

$$(2\pi y)^4 I_{e,3,\mathrm{osc}}(y) \simeq \sum_{n=0} \frac{a_n \lambda^{(9+2n)/4}}{y^{1/2+n}|\lambda^3-1|^{1/2}} \times \cos[2\pi\lambda^{-1/2}y + n\pi/2 + \pi\,\mathrm{sgn}(\lambda-1)/4] + \sum_{n=0} \frac{b_n}{[(\lambda^3-1)y]^{1+n}} \sin(2\pi\lambda y + n\pi/2). \quad (46)$$

Explicit expressions for the coefficients a_n and b_n are given in Appendix *D*.

5.3. Relationship between oscillations in I_d and discontinuities in g and its derivatives

Wu & Schmidt (1974) have reported that discontinuities in g and g' lead to oscillatory components I_{osc} of the type

$$I_{\mathrm{osc}}(s) \propto s^{-4} \sum_k j_k \frac{\sin(2\pi D_k s + \phi_k)}{(2\pi D_k s)^{\mu_k}}, \quad (47)$$

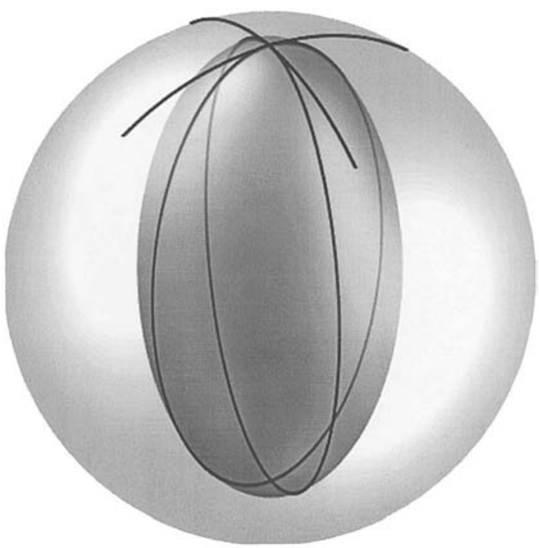

Figure 1
Prolate ellipsoid of revolution (dark) and spherical averaging δ shell (light) touching it at the pole. The principal radii of curvature of the prolate ellipsoid are *both smaller* than the radius of the averaging δ shell.

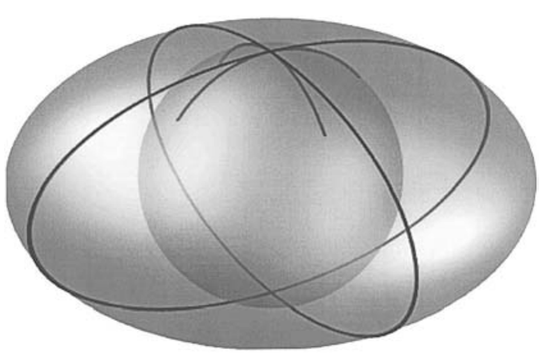

Figure 2
Oblate ellipsoid of revolution (light) and spherical averaging δ shell (dark) touching it at the pole. The principal radii of curvature of the oblate ellipsoid are *both larger* than the radius of the averaging δ shell.

$r = D_k$ is considered to be a position where $g(r)$ or $g'(r)$ has a discontinuity. ϕ_k and j_k are parameters that are determined by the principal curvatures and other properties of the interface at the point of contact of the chord of length D_k. An essential result of their paper is the statement that the exponents μ_k are expected to show values in the range $0 \le \mu_k \le 1$.

The results of §3 offer the possibility of examining this statement.

5.3.1. Integer exponents. Finite discontinuities in $g(r)$ and its derivatives are characterized by the appearance of Dirac δ functions in the next-higher derivative. If, for example, $g^{(n)}(r)$ shows a step of height $\Delta g_k^{(n)}$ at $r = D_k$, then $g^{(n+1)}(r)$ contains a δ function of weight $\Delta g_k^{(n)}$ at $r = D_k$.

Considering the intensity component ΔI_k related to $\Delta g_k^{(n)} = l_p \Delta\gamma_k^{(n+2)}$, we find

$$s^4 \Delta I_k(s) \propto s^{1-n} r_k^2 \Delta g_k^{(n)} K_{d,n+3}^{-1}(z_k), \quad (48)$$

where $z_k = 2\pi D_k s$.

Taking into account that the oscillatory components of $K_{3,n}^{-1}$ are proportional to $z^{-1}\cos z$ and $z^{-2}\sin z$ for odd values of n, and to $z^{-1}\sin z$ and $z^{-2}\cos z$ for even values of n, we find that finite discontinuities in the nth derivative of $g(r)$ result in exponents μ_k with the values n and $n+1$, and that the corresponding phases ϕ_k as defined in (47) can only take the values 0 or $\pi/2$.

Generally, finite discontinuities are located at D_k values which correspond to minimal or maximal dimensions of particles (Wu & Schmidt, 1973*a*). If we consider the method used to derive $\gamma^{(3)}$ in §5.2, finite discontinuities appear when the δ shell of the averaging sphere touches the δ shell of the function $[\gamma^{(3)}(\mathbf{x})]_\delta$ at a distance $r = D_k$ at which the principal radii of curvature (*i.e.* the reciprocal absolute values of the

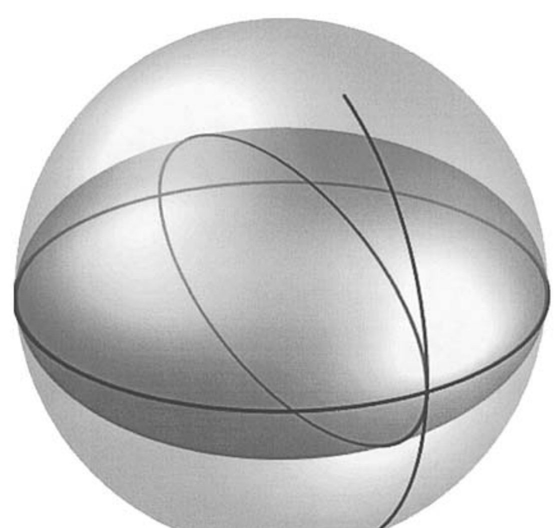

Figure 3
Oblate ellipsoid of revolution (dark) and spherical averaging δ shell (light) touching it at the equator. One principal radius of curvature of the oblate ellipsoid is *equal* to and the other is *smaller* than the radius of the averaging δ shell.

principal curvatures themselves) of the latter are either both smaller (Fig. 1) or both larger (Fig. 2) than D_k.

5.3.2. Non-integer exponents. Non-integer exponents can be related to infinite discontinuities of the type $(1-x)^{\mu_k}$ or $(x-1)^{\mu_k}$, where $\mu_k < 0$ and $x = r/D_k$.

As we have seen in §5.2, infinite discontinuities with $\mu_k = -1/2$ appear when the δ shell of the averaging sphere touches the δ shell of the function $[\gamma^{(3)}(\mathbf{x})]_\delta$ at a distance $r = D_k$ at which one principal radius of curvature of the latter is equal to D_k and the other is either smaller (Fig. 3) or larger (Fig. 4) than D_k. Wu & Schmidt (1974) have shown that this type of discontinuity appears in all convex particles of revolution.

If we use the method given in §5.2 for general ellipsoids, we obtain in $\gamma^{(3)}$, apart from two finite discontinuities at the smallest and the largest diameter, a logarithmic singularity of the type $\ln|1-x|$. This type of singularity has already been discussed by Wu & Schmidt (1973*b*). It should be mentioned that under certain conditions both a finite step and a logarithmic singularity can occur (Ciccariello, 1991*a*,*b*). In $\gamma^{(4)}$, the logarithmic singularity produces a discontinuity of the type $|1-x|^{-1}\,\mathrm{sgn}(1-x)$. The corresponding D_k is defined by the intermediate diameter of the ellipsoid. Thus, infinite discontinuities with integer values of μ_k appear in $\gamma^{(n)}$ with $n > 3$ when the δ shell of the averaging sphere touches the δ shell of the function $[\gamma^{(3)}(\mathbf{x})]_\delta$ at a distance $r = D_k$ at which one principal radius of curvature of the latter is larger and the other is smaller than D_k (see Fig. 5).

These observations suggest that the only non-integer exponents to be expected in the SAS of monodisperse convex particles are of the type $\mu_k = (1+2n)/2$.

5.3.3. Generation of general non-integer exponents. We consider a hypothetical CLD of the type

$$g(x) \propto x(1-x^2)^{\mu}, \qquad (49)$$

where $x = r/D_{\max}$. $g(x)$ is supposed to be non-zero only in the interval $0 \le x \le 1$. We consider μ values larger than zero. For $\mu = 0$, we obtain the CLD of a sphere of diameter $D_{\max}$.

The scattering intensity I $(= I_3)$ corresponding to (49) is given by

$$I(s) = {}_1F_2\left(\begin{matrix} 2 \\ 5/2,\, 4+\mu \end{matrix}\middle| -\frac{z^2}{4}\right), \qquad (50)$$

where z is $2\pi D_{\max} s$. For large values of s, we obtain the asymptote proportional to

$$\frac{1}{z^4} + \frac{a_1}{z^6} + \frac{a_2\cos(z-\mu\pi/2)}{z^{4+\mu}} - \frac{a_3\sin(z-\mu\pi/2)}{z^{5+\mu}} + O\left(\frac{\cos(z-\mu\pi/2)}{z^{6+\mu}}\right), \qquad (51)$$

where the coefficients a_k are functions of μ. If $0 < \mu < 1$, the first derivative

$$g'(x) \propto (1-x^2)^{\mu} - 2\mu x^2(1-x^2)^{\mu-1} \qquad (52)$$

shows an infinite discontinuity at $x = 1$ with an arbitrary non-integer exponent. For larger values of μ, infinite discontinuities appear in the corresponding derivatives of higher order.

It is of interest to note that (49) is equivalent to the CLD of a *polydisperse* dilute system of spheres with a number distribution of diameters h_D of the type

$$h_D(x) \propto x(1-x^2)^{\mu-1}, \qquad (53)$$

where $x = D/D_{\max}$. There is, apparently, *no monodisperse* system of particles corresponding to a chord-length distribution as given by (49).

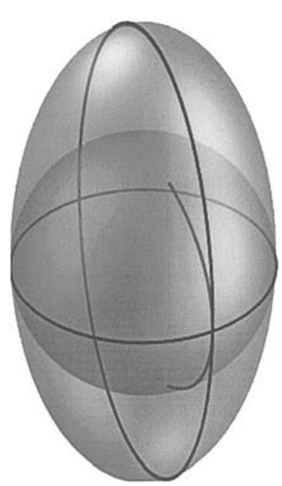

Figure 4
Prolate ellipsoid of revolution (light) and spherical averaging δ shell (dark) touching it at the equator. One principal radius of curvature of the prolate ellipsoid is *equal* to and the other is *larger* than the radius of the averaging δ shell.

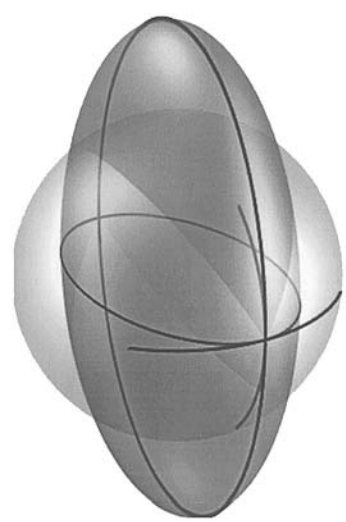

Figure 5
General ellipsoid of revolution (dark) with three different semi-axes $a \ne b \ne c$ and spherical averaging δ shell (light) touching it. One principal radius of curvature of the ellipsoid is *smaller* and the other is *larger* than the radius of the averaging δ shell.

6. Experimental requirements for an accurate determination of CLDs

The determination of $g(r)$ from experimental data requires not only a very high accuracy of the SAS intensity, especially at large s values (Porod asymptote), but also that one is fully aware of all the necessary corrections to be taken into account. These are collimation effects, the subtraction of the scattering due to density fluctuations within the phases, and the elimination of the effect of the finite width of the phase boundaries (Ruland, 1971). Furthermore, the statistical structure of the phase boundaries (Ruland, 1987; Semenov, 1994) can produce supplementary effects. In general, a comprehensive approach taking into account all these effects in a single model which works on the original data and has proper error propagation is preferable to a stepwise application of subsequent corrections where fundamental problems such as ill-posedness and data cut-offs can quickly render the result of one step of the chain meaningless, and usually error propagation is also lost. It is for example highly questionable if any meaningful Porod analysis is still possible after a separate collimation desmearing step. Without a proper treatment of these corrections, the determination of Porod's asymptote is rather arbitrary. In this context, it should be noted that log–log plots of uncorrected intensities *versus* s produce, in many cases, fractional exponents which can be misinterpreted as the scattering from fractal structures (Ruland, 2001).

APPENDIX *A*
Derivation of the inverse kernel

We assume $\gamma(r)$ to be defined for positive values of r only, and continuously differentiable at $r = 0$. We consider the integral transform

$$\gamma^{(n)}(r) = \int_v (2\pi s)^n I_d(s) K_d^{(n)}(z)\, \mathrm{d}v_{d,s}, \qquad (54)$$

where the kernel is given by

$$K_d(z) = \Gamma(d/2)(z/2)^{1-d/2} J_{d/2-1}(z), \qquad (55)$$

with $z = 2\pi rs$ and

$$\mathrm{d}v_{d,s} = \frac{2\pi^{d/2}}{\Gamma(d/2)} s^{d-1}\, \mathrm{d}s \qquad (56)$$

is the volume element in reciprocal space. We want to determine the inverse kernel $K_{d,n}^{-1}$ with the property

$$(2\pi s)^n I_d(s) = \int_v \gamma^{(n)}(r) K_{d,n}^{-1}(z)\, \mathrm{d}v_{d,r}, \qquad (57)$$

where

$$\mathrm{d}v_{d,r} = \frac{2\pi^{d/2}}{\Gamma(d/2)} r^{d-1}\, \mathrm{d}r. \qquad (58)$$

The relationship between the kernels can be defined by

$$\int_0^\infty K_d^{(n)}(2\pi rs') \frac{2\pi^{d/2}}{\Gamma(d/2)} (s')^{d-1} \times K_{d,n}^{-1}(2\pi rs) \frac{2\pi^{d/2}}{\Gamma(d/2)} r^{d-1}\, \mathrm{d}r = \delta(s - s'). \qquad (59)$$

A closed-form solution for arbitrary n can be obtained by representing $K_d^{(n)}(z)$ as a Meijer's G function

$$K_d(z) = {}_0F_1\left(\frac{d}{2}\middle| -\frac{z^2}{4}\right) = \Gamma\left(\frac{d}{2}\right) G_{02}^{10}\left(\frac{z^2}{4}\middle| 0, 1 - d/2\right) \qquad (60)$$

$$K_d^{(n)}(z) = (-1)^n \Gamma(d/2) \times G_{13}^{20}\left(\frac{z^2}{4}\middle| \begin{matrix} (1-n)/2 \\ 0, 1/2, 1-(d+n)/2 \end{matrix}\right), \qquad (61)$$

where the derivative order n now is an arbitrary parameter.

The integral of the product of two G functions results in another G function. Dirac's δ function can be represented by G_{00}^{00}. The inverse kernel is assumed to be representable by a G function, the coefficients of which have to be determined such that all parameters of G vanish in the result of (59). This is the case for

$$K_{d,n}^{-1}(z) = (-1)^n \Gamma(d/2) G_{13}^{11}\left(\frac{z^2}{4}\middle| \begin{matrix} (1-d+n)/2 \\ n/2, (1-d)/2, 1-d/2 \end{matrix}\right) = \frac{(-z)^n}{(d)_n}\, {}_1F_2\left(\begin{matrix} (1+d)/2 \\ (d+n)/2, (1+d+n)/2 \end{matrix}\middle| -\frac{z^2}{4}\right). \qquad (62)$$

APPENDIX *B*
Alternative derivation of the inverse kernel

For $d = 1$, an equivalent expression can be obtained by considering the complete function γ_c defined by

$$\gamma_c(r) = \gamma(|r|). \qquad (63)$$

Using Fourier transform theory, we find

$$\gamma_c^{(n)}(r) = \int_{-\infty}^{\infty} (2\pi s)^n I_1(s) \cos^{(n)}(z)\, Z\, \mathrm{d}s \qquad (64)$$

$$(2\pi s)^n I_1(s) = \int_{-\infty}^{\infty} \gamma_c^{(n)}(r) \cos^{(n)}(z)\, \mathrm{d}r. \qquad (65)$$

For $m \geq 1$, the derivatives of $\gamma_c(r)$ are given by

$$\gamma_c^{(2m)}(r) = \gamma^{(2m)}(|r|) + 2 \sum_{k=0}^{m-1} \gamma^{(2m-2k-1)}(0) \delta^{(2k)}(r) \qquad (66)$$

$$\gamma_c^{(2m-1)}(r) = \gamma^{(2m-1)}(|r|)\, \mathrm{sgn}(r) + 2 \sum_{k=1}^{m-1} \gamma^{(2m-2\,k-1)}(0) \delta^{(2k-1)}(r). \qquad (67)$$

This results in

$$(2\pi s)^{2m} I_1(s) = 2(-1)^m \left[\int_0^\infty \gamma^{(2m)}(r) \cos(z)\, \mathrm{d}r + \sum_{k=0}^{m-1} (-1)^k (2\pi s)^{2k} \gamma^{(2m-2k-1)}(0) \right] \quad (68)$$

$$(2\pi s)^{2m-1} I_1(s) = 2(-1)^m \left[\int_0^\infty \gamma^{(2m-1)}(r) \sin(z)\, \mathrm{d}r + \sum_{k=1}^{m-1} (-1)^k (2\pi s)^{2k-1} \gamma^{(2m-2k-1)}(0) \right]. \quad (69)$$

It can be shown that the above expressions are equivalent to

$$(2\pi s)^n I_1(s) = \int_v \gamma^{(n)}(r) K_{1,n}^{-1}(z)\, \mathrm{d}v_{1,r}, \quad (70)$$

provided that

$$\int_0^\infty \gamma^{(2m)}(r)\, \mathrm{d}r = -\gamma^{(2m-1)}(0), \quad (71)$$

i.e.

$$\gamma^{(2m-1)}(\infty) = 0. \quad (72)$$

The latter condition has to be considered as a criterion of convergence for $\gamma(r)$.

Comparable results can be found for other values of d using relationships of the type

$$I_3(s) = -\frac{1}{2\pi s} \frac{\partial}{\partial s} I_1(s) \quad (73)$$

$$I_2(s) = 2 \int_0^\infty I_3(s^2 + y^2)^{1/2}\, \mathrm{d}y. \quad (74)$$

APPENDIX *C*
Asymptotic expansion of the inverse kernel

The asymptotic expansion of the inverse kernel $K_{d,n}^{-1}$ is split into a non-oscillatory and an oscillatory component:

$$K_{d,n}^{-1} = K_{d,n,\mathrm{nos}}^{-1} + K_{d,n,\mathrm{osc}}^{-1}. \quad (75)$$

For the non-oscillatory part, we find

$$K_{d,n,\mathrm{nos}}^{-1}(z) = (-1)^n \frac{\Gamma(d)}{\Gamma(n-1)} z^{-1-d+n} \times {}_3F_0\left(\frac{1+d}{2}, 1-\frac{n}{2}, \frac{3-n}{2} \middle| -\frac{4}{z^2} \right). \quad (76)$$

For $n = 0$ or $n = 1$, this expression vanishes identically due to the diverging Γ function in the denominator of the prefactor. Thus, there are no non-oscillatory parts for $n < 2$.

Since n is an integer, one of the parameters of the ${}_3F_0$ function always becomes a negative integer. Thus, the hypergeometric function reduces to a polynomial in z^{-2} of the order $(n-2)/2$ for even n and $(n-3)/2$ for odd n, respectively. Explicitly, we find

$$K_{d,n,\mathrm{nos}}^{-1}(z) = (-1)^{1+n} \frac{\Gamma(d)}{n!} z^{-1-d+n} n(1-n) \times \left\{ 1 - \left(\frac{1+d}{2}\right)(2-n)(3-n)z^{-2} + \left(\frac{1+d}{2}\right) \times \left(\frac{3+d}{2}\right)(2-n)(3-n)(4-n)(5-n)\frac{z^{-4}}{2!} + O(z^{-6}) \right\}. \quad (77)$$

The building law of this expression and its termination are obvious.

For the oscillatory component of the asymptotic expansion of the inverse kernel $K_{d,n}^{-1}$, we find

$$K_{d,n,\mathrm{osc}}^{-1}(z) = (-1)^n \pi^{-1/2} \Gamma(d/2)(2/z)^{(d-1)/2} \times \left\{ \cos[z - \pi(d-1+2n)/4] + \frac{(d-1)(d+4n-3)}{8z} \cos[z - \pi(d-3+2n)/4] + O((d-3)\ldots z^{-2} \cos[z - \pi(d-5+2n)/4]) \right\}. \quad (78)$$

This series terminates for $d = 1$ after the first and for $d = 3$ after the second term, respectively. It can be shown that, when both the non-oscillatory and the oscillatory series of the asymptotic expansion terminate, the asymptotic expansion is equal to the exact solution. Thus, for odd values of d, the inverse kernel can be expressed in simple trigonometric form, see Table 1. The same behavior is found *e.g.* in Bessel functions $J_{d/2}$, which have a simple trigonometric representation for odd integer d.

For an even d including $d = 2$, the asymptotic expansion (78) has an infinite number of terms. This case is more complicated and the exact solution cannot be expressed in trigonometric form. However, it can be represented in terms of Bessel and Struve functions of the first kind of integer orders. Explicit expressions are listed in Table 2.

APPENDIX *D*
Asymptotic behavior of the ellipsoid of revolution

The function $I_{e,\mathrm{osc}}$ of the ellipsoid of revolution is composed of the real and the imaginary parts, respectively, of the components J_k

$$(2\pi y)^4 I_{e,\mathrm{osc}}(y) = \mathrm{Re}[J_1 + J_3] + \mathrm{Im}[J_2], \quad (79)$$

where the functions $J_k(y)$ are the Fourier transforms of $f_k(x)$,

$$J_k = \int_{\lambda^{-1/2}}^{\lambda} f_k(x) \exp(2\pi i x y)\, \mathrm{d}x \quad (80)$$

and

Table 3
The coefficients a_n and b_n defined in (88) of the asymptotic expansion of the ellipsoid of revolution.

n	a_n	b_n
0	6π	$6/\lambda^2$
1	$57/2^3$	$-3/(\lambda^3\pi)$
2	$243/(2^8\pi)$	$3(4\lambda^3-1)/(2\pi^2\lambda)$
3	$1899/(2^{12}\pi^2)$	$-9(8\lambda^6-4\lambda^3+1)(4\pi^3\lambda^2)^{-1}$
4	$-335007/(2^{18}\pi^3)$	$9(56\lambda^9-36\lambda^6+19\lambda^3-4)(8\pi^4\lambda^3)^{-1}$
5	$13746375/(2^{22}\pi^4)$	$-9(448\lambda^{12}-304\lambda^9+264\lambda^6-113\lambda^3+20)/(16\pi^5\lambda^4)$

$$f_1(x) = -4\pi x[\gamma_e^{(3)}(x)]_\delta \tag{81}$$

$$f_2(x) = \frac{8}{y}[\gamma_e^{(3)}(x)]_\delta \tag{82}$$

$$f_3(x) = \frac{4}{\pi x y^2}[\gamma_e^{(3)}(x)]_\delta . \tag{83}$$

The Fourier transforms can be obtained as an asymptotic expansion according to Erdélyi (1956) of the type

$$J_k = B_{k,N} - A_{k,N} + O(y^{-N}), \tag{84}$$

where

$$\begin{aligned} A_{k,N} = &-\sum_{n=0}^{N-1} \frac{\Gamma(n+1/2)}{n!(2\pi y)^{n+1/2}|\lambda^3-1|^{1/2}} \\ &\times \exp\{i(2\pi\lambda^{-1/2}y + n\pi/2 + \pi\,\mathrm{sgn}[\lambda-1]/4)\} \\ &\times \left[\frac{\partial^n}{\partial x^n}\Phi_k(x)\right]_{x=\lambda^{-1/2}} \end{aligned} \tag{85}$$

$$\begin{aligned} \Phi_k(x) = &(x-\lambda^{-1/2})^{1/2}|\lambda^3-1|^{1/2} \\ &\times \exp\{\pi i(1-\mathrm{sgn}[\lambda-1])/4\} f_k(x) \end{aligned} \tag{86}$$

$$\begin{aligned} B_k, N = &\sum_{n=0}^{N-1}(2\pi y)^{-n-1}\exp\{i(2\pi\lambda y + \pi[n-1]/2)\} \\ &\times \left[\frac{\partial^n}{\partial x^n} f_k(x)\right]_{x=\lambda}. \end{aligned} \tag{87}$$

The result is

$$\begin{aligned} (2\pi y)^4 I_{e,\mathrm{osc}}(y) \simeq &\sum_{n=0} \frac{a_n\lambda^{(9+2n)/4}}{y^{n+1/2}|\lambda^3-1|^{1/2}} \\ &\times \cos(2\pi\lambda^{1/2}y + n\pi/2 + \pi\,\mathrm{sgn}[\lambda-1]/4) \\ &+ \sum_{n=0}\frac{b_n}{[(\lambda^3-1)y]^{1+n}}\sin(2\pi\lambda y + n\pi/2). \end{aligned} \tag{88}$$

The first six coefficients of expansion (88) are shown in Table 3.

APPENDIX *E*
Application of the inverse kernel to one-dimensional and two-dimensional two-phase systems

In our treatment so far, we considered a three-dimensional isotropic two-phase system, and the spatial dimension d described the projection the corresponding intensity distribution was subject to. Let us limit the following considerations to the unprojected (unsmeared) case, but consider two-phase systems of lower dimension, namely systems of infinitely high cylinders or prisms ($d = 2$) and systems of infinitely extended lamellae ($d = 1$). In these lower-dimensional two-phase systems, we are interested in the CFs γ_d, the CLDs $g_d \propto \gamma_d''$ and the intensity distributions I_d of the two-dimensional cross section perpendicular to the cylinders or the one-dimensional section in the direction of the lamella normals, respectively

$$I_d(s) = \int_v \gamma_d(r) K_d(z)\,\mathrm{d}v_{d,r}, \tag{89}$$

which is different from the overall three-dimensional CLD of the spherically averaged system. A spherical average of I_d leads to

$$I(s) = \left\{\begin{matrix} \langle\delta(s_1)\delta(s_2)I_1(s_3)\rangle_\omega \\ \langle I_2(s_{12})\delta(s_3)\rangle_\omega \\ I_3(s)\end{matrix}\right\} = \left\{\begin{matrix} (2\pi s^2)^{-1}I_1(s) \\ (2s)^{-1}I_2(s) \\ I_3(s)\end{matrix}\right\} = \frac{\pi^{d/2-1}s^{d-3}}{2\Gamma(d/2)}I_d(s). \tag{90}$$

The inverse kernel derived in this paper allows us to establish a relationship between the (in pinhole collimation) experimentally measured spherically averaged intensity I and the subdimensional CLDs γ_d'' and their higher derivatives $\gamma_d^{(n)}$.

$$\gamma_d(r) = \int_v I_d(s) K_d(z)\,\mathrm{d}v_{d,s} \tag{91}$$

$$\begin{aligned} \gamma_d^{(n)}(r) &= \int_v (2\pi s)^n I_d(s) K_d^{(n)}(z)\,\mathrm{d}v_{d,s} &(92) \\ &= \int_v (2\pi s)^n \frac{2\Gamma(d/2)}{\pi^{d/2-1}s^{d-3}} I(s) K_d^{(n)}(z)\,\mathrm{d}v_{d,s} &(93) \end{aligned}$$

and the inversion is

$$2^{1+n}\Gamma(d/2)\pi^{1+n-d/2}s^{3-d+n}I(s) = \int_v \gamma_d^{(n)}(r) K_{d,n}^{-1}(z)\,\mathrm{d}v_{d,r}. \tag{94}$$

It is even possible to combine a subdimensional two-phase system with a projection of the intensity distribution, but in this case the general inverse kernel can only be given in terms of a Meijer's G function that cannot be further simplified.

References

Ciccariello, S. (1991*a*). *Phys. Rev. A*, **44**, 2975–2983.
Ciccariello, S. (1991*b*). *J. Appl. Cryst.* **24**, 509–515.
Ciccariello, S. (1993). *Acta Cryst.* A**49**, 398–405.
Ciccariello, S. (1995). *J. Math. Phys.* **36**, 219–246.
Ciccariello, S. & Benedetti, A. (1982). *Phys. Rev. B*, **26**, 6384–6389.
Ciccariello, S., Cocco, G., Benedetti, A. & Enzo, S. (1981). *Phys. Rev. B*, **23**, 6474–6485.
Ciccariello, S. & Sobry, R. (1995). *Acta Cryst.* A**51**, 60–69.
Erdélyi, A. (1956). *Asymptotic Expansions*, pp. 49–50. New York: Dover.
Kirste, R. G. & Porod, G. (1962). *Kolloid Z.* **184**, 1–7.
Méring, J. & Tchoubar, D. (1968). *J. Appl. Cryst.* **1**, 153–165.
Méring, J. & Tchoubar-Vallat, D. (1965). *C. R. Acad. Sci.* **261**, 3096–3099.

Méring, J. & Tchoubar-Vallat, D. (1966). *C. R. Acad. Sci.* **262**, 1703–1706.
Porod, G. (1951). *Kolloid Z.* **124**, 83–114.
Porod, G. (1952*a*). *Kolloid Z.* **125**, 51–57.
Porod, G. (1952*b*). *Kolloid Z.* **125**, 109–122.
Porod, G. (1967). *Small-Angle Scattering of X-rays*, edited by H. Brumberger, pp. 1–15. New York/London/Paris: Gordon and Breach.
Ruland, W. (1971). *J. Appl. Cryst.* **4**, 70–73.
Ruland, W. (1977). *Colloid Polym. Sci.* **255**, 417–427.
Ruland, W. (1978). *Colloid Polym. Sci.* **256**, 932–936.
Ruland, W. (1987). *Macromolecules*, **20**, 87–93.
Ruland, W. (2001). *Carbon*, **39**, 323–324.
Semenov, A. N. (1994). *Macromolecules*, **27**, 2732–2735.
Sobry, R., Fontaine, F. & Ledent, J. (1994). *J. Appl. Cryst.* **27**, 482–491.
Wu, H. & Schmidt, P. W. (1971). *J. Appl. Cryst.* **4**, 224–231.
Wu, H. & Schmidt, P. W. (1973*a*). *Monatsh. Chem.* **104**, 784–799.
Wu, H. & Schmidt, P. W. (1973*b*). *J. Appl. Cryst.* **6**, 66–72.
Wu, H. & Schmidt, P. W. (1974). *J. Appl. Cryst.* **7**, 131–146.